

Article

Evaluating the Increasing Trend of Strength and Severe Wind Hazard of Philippine Typhoons Using the Holland-B parameter and Regional Cyclonic Wind Field Modeling

Joshua Agar ^{1*}¹ Institute of Civil Engineering, University of the Philippines; jcagar@up.edu.ph

* Correspondence: jcagar@up.edu.ph; Tel.: (+63) 922 815 4622

Abstract: For the Philippines, a country exposed to multiple natural hazards like severe wind, sustainable development includes resiliency. Severe wind hazard is brought by tropical cyclones in the Western Pacific, known as typhoons, that frequent the Philippines. Therefore, adequately evaluating the wind hazard and its impact is crucial for sustainable building design. Acknowledging the impacts of climate change on said hazards would require adaptation to its consequences which necessitate a deeper understanding on the changing behavior of typhoons in recent years. For this study, detailed wind information from the Japan Meteorological Agency from 1977-2021, the Holland-B parameter, and the radius of maximum wind speed for each typhoon, are determined for simulation of the regional cyclonic wind field. The analysis of the Holland-B parameters, which represent the steepness of the pressure gradient and tropical cyclone convection, suggest that the Holland-B parameters have been increasing since 2011. The regional wind fields caused by the typhoons also suggest an increasing trend in severe wind hazard. Seasonality for the location of severe wind hazard is also observed, with the Southern Philippines experiencing an increase (decrease) during the Northeast (Southwest) Monsoon season, and the Northern Philippines experiencing an increase (decrease) during the Southwest (Northeast) Monsoon season.

Keywords: Holland-B Parameter; Philippine typhoons; Regional wind; Wind hazard

1. Introduction

Severe wind is one of the hazards that pose a risk to the integrity and sustainability of buildings in the Philippines. The Philippines, through its weather agency, the Philippine Atmospheric, Geophysical, and Astronomical Services Administration or PAGASA, has been monitoring the severe wind hazard primarily brought by typhoons which enter what's called the Philippine Area of Responsibility or PAR. An average of 20 typhoons enter PAR on which an average of 10 typhoons make landfall [1].

PAGASA uses the meteorological standard of 10-minute sustained wind speeds in identifying typhoons into five categories in 2022: tropical depressions which have 10-minute sustained winds between 55 kph and 61 kph, tropical storms which have 10-minute sustained winds between 62 kph to 88 kph, severe tropical storms which have 10-minute sustained winds between 89 kph and 117 kph, typhoons which have 10-minute sustained winds between 118 kph and 184 kph, and super typhoons which have 10-minute sustained winds of greater than 185 kph. Originally with three (3) warning systems in 1970, the PAGASA issues Public Storm Warning Signals which have been then revised, with the inclusion of Public Storm Warning Signal No. 4 (>185 kph) in 1991 as a result of Typhoon Mike in 1990 [2] and the inclusion of Public Storm Warning Signal No.5 (>220 kph) in 2015 as a result of Typhoon Haiyan in 2013 [3]. With the 2022 reclassification of typhoons, the Public Storm Warning Signals are adjusted based on the recent category [4].

The reclassification and the updates on the public storm warning signals are done to meet the risk posed by typhoons as part of the disaster risk reduction management

(DRRM). The Kyoto Protocol [5] and the Paris agreement [6] have acknowledged the need to address climate change and have made necessary commitments to meet the targets to mitigate the risk.

DRRM experts are asked whether climate change will affect typhoons as policy-making requires adaptation particularly in sustainable development and building design. The Intergovernmental Panel on Climate Change (IPCC) has reported back in 2001 that there are some increases in tropical cyclone maximum intensities [7], although years prior, there were no discernible trends in increase in typhoon numbers and intensities from historical analysis [8]. Estimates in 2004 suggested an increase by 5% to 10% by 2050 [9]. Treading upon this topic, however, requires caution. In 2017, a projection shows an increasing intensity to tropical cyclones across different basins with the exception of the Western Pacific typhoons [10]. However, it has been noted that wind speed measurements in the 1940s and the 1960s in the Western Pacific basin were too strong [11]. A subsequent analysis by the IPCC in 2020 shows that despite the lack of increase in the number of typhoons, the typhoons increase in intensity, that intense typhoons increase in numbers, and that the typhoon precipitation also increases [12].

The known sources of uncertainty for future typhoon projections include sea surface temperature uncertainty, vertical temperature gradient of upper ocean [13], typhoon cyclogenesis, and atmospheric circulation changes. The question on those uncertainties are further pressed with the Typhoon Rai (PAGASA Name: Odette) in 2021 which became the 2nd costliest typhoon in Philippine history. Typhoon Rai underwent rapid intensification, identified as the 95th percentile increase of maximum winds within a 24-hr period. Regions of rapid intensification were identified to have been occurring east of the Philippines, frequently before landfall, which has been attributed to the changes in the sea surface temperatures, which the models cannot predict at that time [14].

Typhoon Rai is one of the December typhoons whose numbers have been on the rise in the past 10 years. Mindanao Island, which it struck, experienced a 480% increase of typhoon passage. The increase of these December typhoons and the increase of probability of Southern Philippines experiencing typhoon passage are attributed to the favorable large scale sea surface conditions due to the positive shift of the Pacific Decadal Oscillation (PDO) [15]. The westward track of typhoons to the Philippines are also attributed to the Western Pacific Subtropical High (WPSH). Both the positive PDO and the stronger and more southern WPSH [16] resulted in large scale environments that are favorable to tropical cyclones. The PDO is a decadal event while the WPSH has seasonal characteristics. The variability of the WPSH is closely related to the onset of both the Southwest Monsoon season – which happens in the months of June, July, August, and September – and the Northeast Monsoon season – which happens in the months of October, November, and December. Evaluating the cyclogenesis of typhoons between 1985-2010 reveal that typhoons, which are wetter, form closer to the Philippines during the Southwest Monsoon season while typhoons, which are drier, originate farther at sea during the Northeast Monsoon season [17]. Typhoons tend to move peripherally with respect to the southern and western sections of WPSH. The increase of intensity and a westward shift of the WPSH result in typhoons forming at lower latitudes and presuming a more westward track while otherwise resulting in from a northwest to a northeast recurving pattern of typhoons [18] [19].

With the change of characteristic and behavior of typhoons due to climate change identified, what remains is the evaluation of the trend on severe wind hazard that typhoons are causing in the Philippines. This study aims to identify the changes in the wind hazard of typhoons in the Philippines by evaluating the changes in the regional cyclonic wind fields [20] with the Philippine Area of Responsibility. The identification of these changes in the wind hazard could prompt policy-makers and engineers to reconfigure their building design and disaster risk reduction and management measures to ensure sustainability that adapts to the changes of the climate.

2. Materials and Methods

2.1. Tropical Cyclone Modeling

For this study, the detailed wind information data of typhoons by Japan Meteorological Agency (JMA) was used. The data, spanning from 1977 to 2021, include maximum sustained winds, minimum central pressures, radii of storm winds, radii of gale winds, and storm track (Figure 1) of each recorded typhoon.

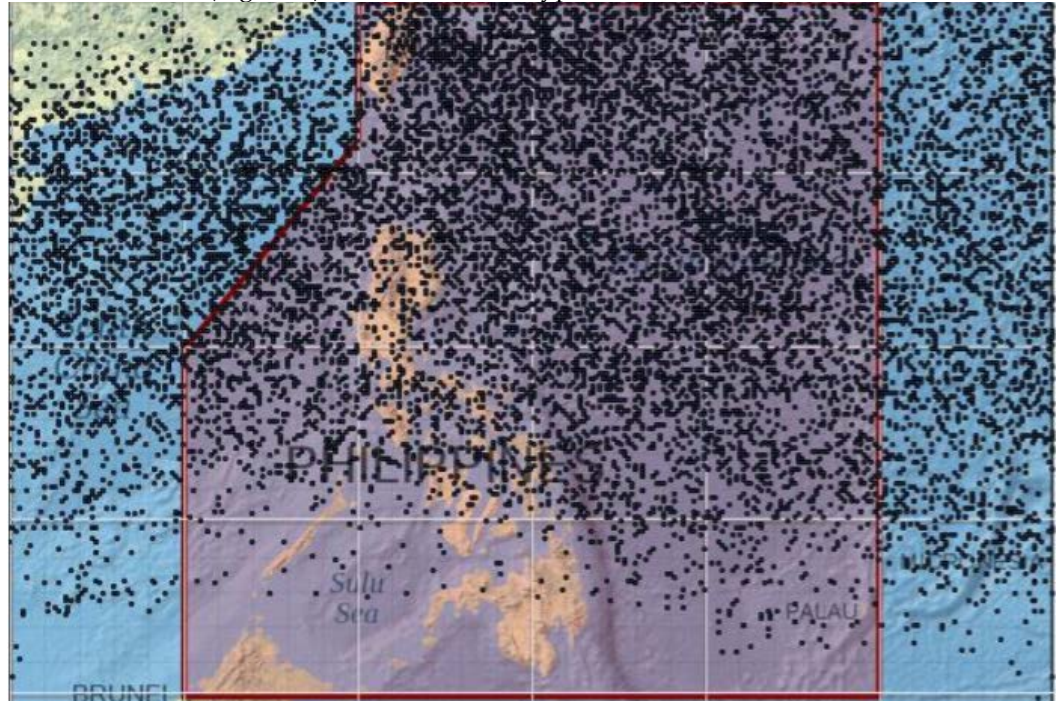


Figure 1. Tracks of all typhoons passing through the Philippines from 1977-2021.

To model the horizontal wind profile, the estimation of the horizontal pressure profile must be conducted first. The pressure profile of typhoons resembles a rectangular hyperbola represented by shape parameters A and B [21], with B being known as the Holland-B parameter [22] [23]:

$$B = \frac{V_{max}^2}{\rho e(p_n - p_0)} \quad (1)$$

Where V_{max} is the maximum gradient wind in m/s, ρ is the density of air in kg/m³, p_n is the ambient pressure assumed to be 1013 hPa, and p_0 is the minimum central pressure of the typhoon in hPa.

Obtaining the pressure profile results in determining the pressure gradient which is one of the three main forces, neglecting surface friction and apart from Coriolis force and Centrifugal force due to the curvature of the motion of the parcel of air intending to move parallel to the curving pressure isobars. This results to a horizontal wind profile equation:

$$V(r) = -\frac{fr}{2} + \sqrt{\left(\frac{fr}{2}\right)^2 + V_{max}^2 \left(\frac{R_{max}}{r}\right)^B e^{-\left(\frac{R_{max}}{r}\right)^B}} \quad (2)$$

Where $V(r)$ is the gradient wind speed at distance r from the center of the typhoon, f is the Coriolis parameter which is a function of the latitude, R_{max} is the radius of maximum winds which is also related to the shape function A [22].

$$A = R_{max}^{1/B} \quad (3)$$

R_{\max} and A can be computed by considering the radius of storm winds and radius of gale winds identified by JMA in the detailed wind information. Knowing that gale winds constitute to winds greater than 62 kph and storm winds constitute to winds greater than 89 kph [24], the gale winds and the storm winds can serve as the isotach to find the value for R_{\max} and A , shown in Figure 2.

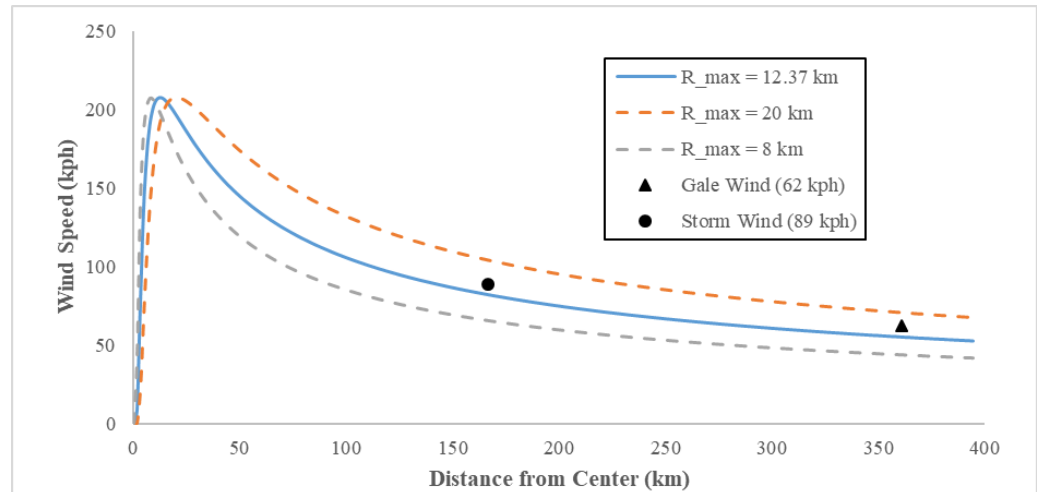


Figure 2. Determining R_{\max} using the detailed wind information for the gale wind and storm wind.

2.2. Regional Wind Field Modeling

Since the forces involved don't include friction in the resulting horizontal wind profile, effects of turbulence are factored out, hence the winds are regional wind speeds which are assumed to be 10-minute sustained winds. With the method of analysis being done with respect to the center of the storm, for the stationary observer, the resulting regional wind speed is computed:

$$\vec{V}_{10-\min}(r) = \vec{V}_{\text{gradient}}(r) + \vec{V}_{\text{translation}} \quad (4)$$

Where $V_{10-\min}(r)$ is the 10-minute sustained wind at distance r from the center of the typhoon, $V_{\text{gradient}}(r)$ is a gradient wind computed using Equation (2), and $V_{\text{translation}}$ is translational velocity of the typhoon.

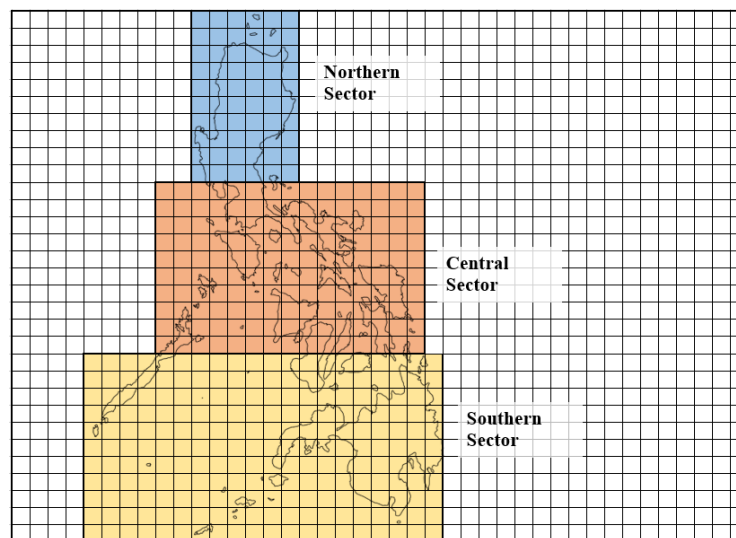


Figure 3. Grid Setup for the Regional Cyclonic Wind Field Simulation

A total of 1148 typhoons (tropical storms and stronger) from 1977 to 2021 are subjected to the tropical cyclone modeling procedure, processing a total of 42744 detailed wind information data, interpolating the 6-hourly and 3-hourly detailed wind information data and storm track to 1-hour intervals resulting to what's called the regional cyclonic winds, since they're free from surface friction and they're cyclonic in nature. This study will focus on the regional cyclonic wind field, as the surface wind is more dependent on wind exposure which involves topography, vegetation, and human settlement and wind exposure varies throughout the Philippines and is different at sea and on land. Regional cyclonic wind fields are assumed to be independent of wind exposure [25] and are assumed to coincide with the 10-minute sustained winds.

The regional cyclonic wind field is simulated over 961 stationary observation points which are arranged in a 0.5-degree-by-0.5-degree grid from 5°N to 20°N and from 115°E to 135°E, shown in Figure 3. Each observation point will contain a total of 131,704 hourly simulated regional cyclonic wind field data with an example shown in Figure 4.

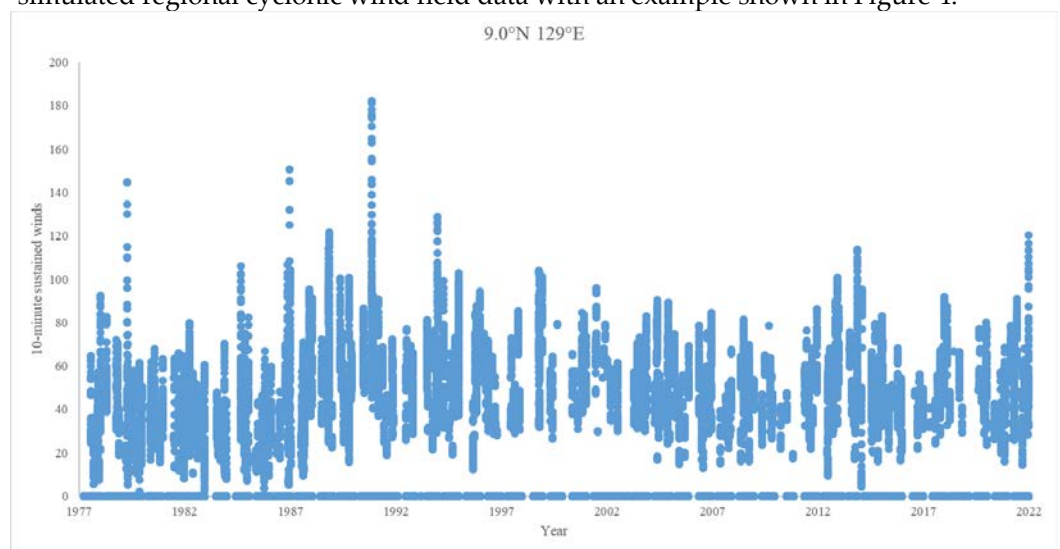


Figure 4. Hourly Simulated Regional Cyclonic Wind Field Data

2.3. Return Period Analysis

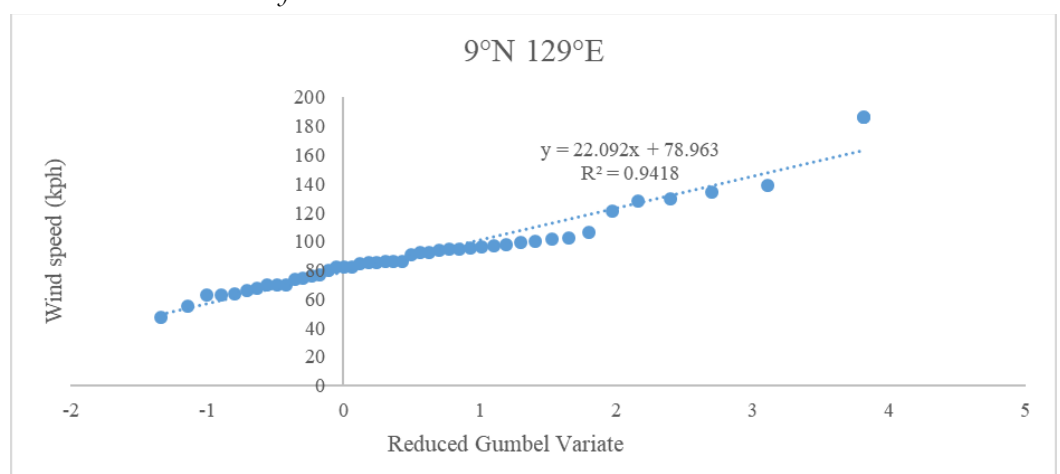


Figure 5. Fitting of Generalized Extreme Value Function

With the annual and monthly maxima being obtained from each observation point, an extreme value (GEV) analysis is being done to determine the return period winds. The annual maxima at each observation point are fitted into a generalized extreme value (GEV) function using Type I distribution [26] [27].

$$V(R) = u + a \left(-\ln \left(-\ln \left(1 - \frac{1}{R} \right) \right) \right) \quad (5)$$

Where u and a are the generalized extreme value function coefficients and $V(R)$ is the return period wind speed at a return period of R years.

To determine how the recent data have resulted in the changes in the return period winds, for each observation point the GEV analysis is done to the regional cyclonic winds from 1977-2010 and the other GEV analysis is done to the regional winds from 1977-2021. The 100-year winds for both GEV analysis are compared.

2.4. Historical Analysis

Apart from the return period winds, the historical maxima of the period of 1977-2010 and 2000-2010 are compared with the historical maxima of the period of 2011-2021 to determine how the maxima have changed over different sectors of the Philippines described in Figure 3. The maxima of the Southwest Monsoon months – which are composed of the months of June, July, August, and September – and the Northeast Monsoon months – which are composed of the months of October, November, and December – of the two different periods are also compared to determine the changes in the seasonal variations of the wind hazard brought by typhoons.

2.5. ENSO Analysis

The computed Holland-B parameters are then related to the sea-surface temperature (SST) anomalies of the El Niño-Southern Oscillation (ENSO) as studies have shown that a necessary condition for development lies on the SST anomalies which coincide with the observed sea level pressure difference between Tahiti and Darwin, Australia standardized into the Southern Oscillation Index (SOI) [28] [29]. The Holland-B parameters of typhoons are specifically related to the warm and cold phases of SOI which indicates the onset of El Niño and La Niña.

3. Results

3.1. Timeline of Holland B Parameter of Typhoons

The timeline of the Holland-B parameter of typhoons are determined and shown in Figure 6. It is important also to take note that there is a shift from the reconnaissance mission measurements to the satellite measurements after 1987.

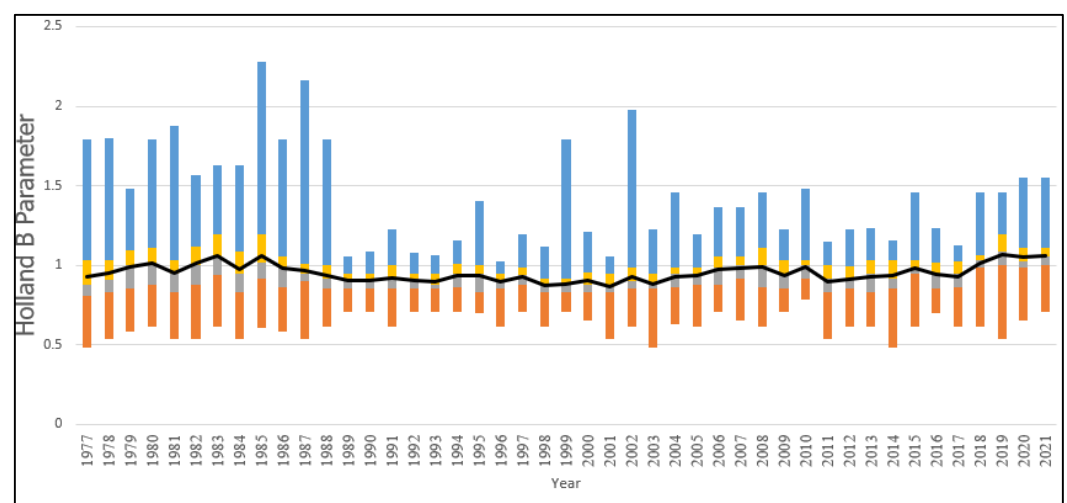


Figure 6. Time history of the Box Plots of the Holland-B Parameters of Typhoons from 1977-2021

3.2. SOI vs Holland-B Parameter

The Holland-B parameters for the typhoon present at a certain month are correlated to the Southern Oscillation Index determined during that month. Compilation of the correlation results in the box plot shown in Figure 7.

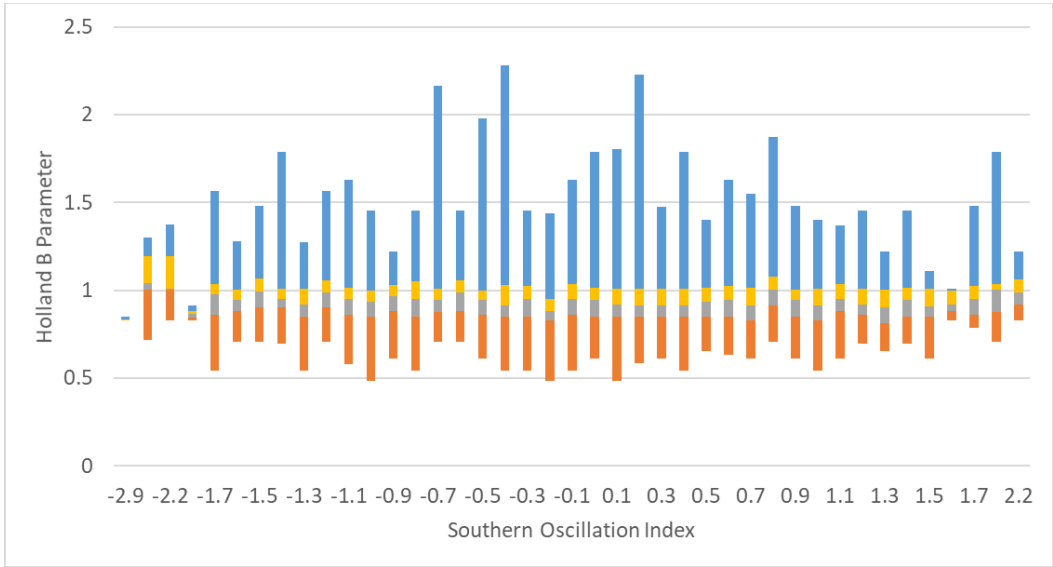


Figure 7. Box Plots of the Holland-B Parameters of Typhoons with respect to SOI

3.3. Changes in the Annual Maximum Winds

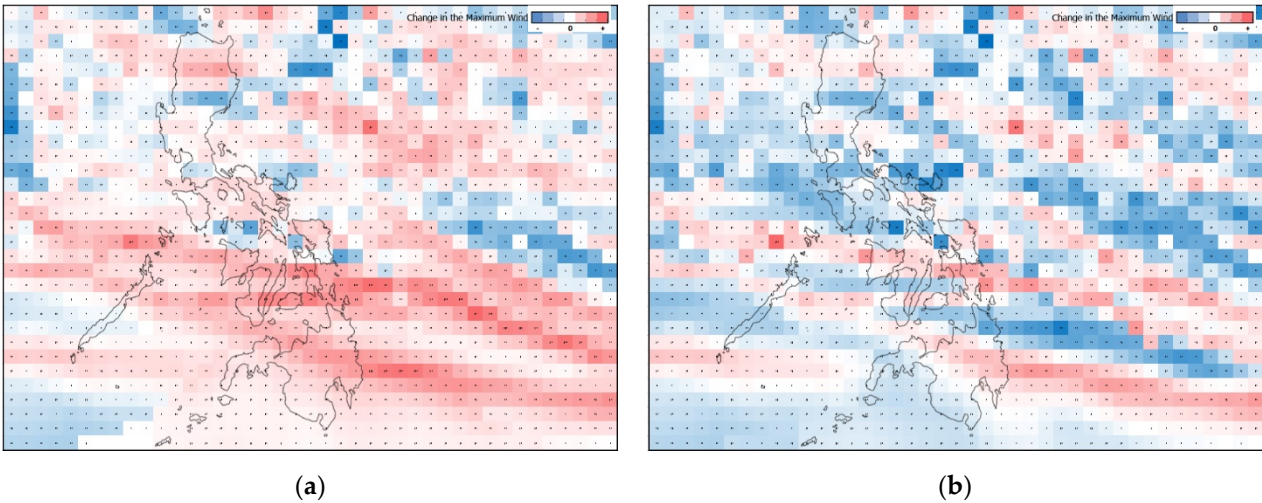


Figure 8. Net Difference of Maximum Year-round Winds (a) 2011-2021 vs 2000-2010 (b) 2011-2021 vs 1977-2010

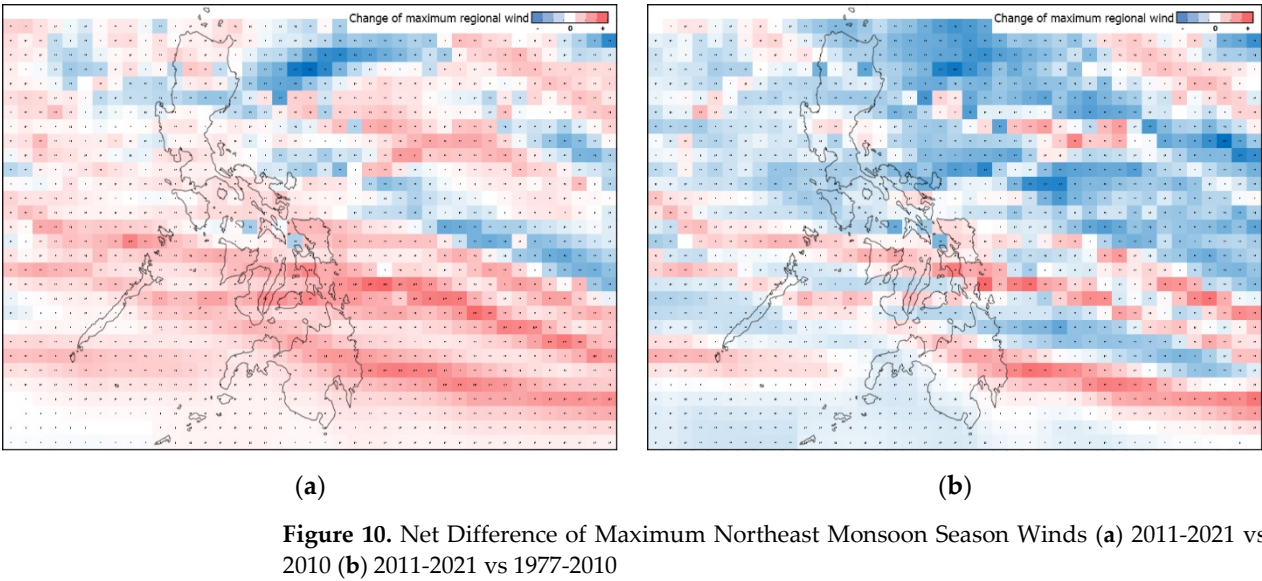
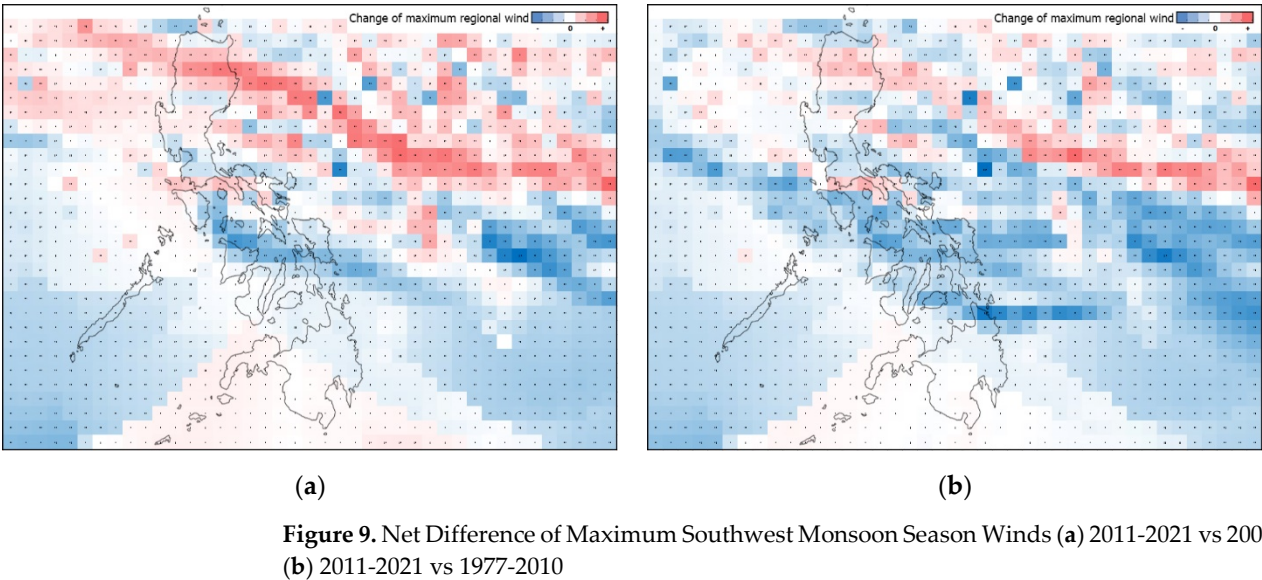
The maximum winds determined during the period of 2011-2021 are compared with the maximum winds determined during the period of 2000-2010 to limit the time when the JMA is in charge of the Western Pacific Basin. The comparison is done to year-round maximum winds, Southwest Monsoon season maximum winds, and Northeast Monsoon maximum winds. To also compare with the overall period to include when the Joint Typhoon Warning Center was in charge of the Western Pacific Basin, the maximum winds determined during the period of 2011-2021 are also compared with the maximum winds determined during the period of 1977-2010. The percent change of maximum winds between the period of 2000-2010 and the period of 2011-2021 and between the period of 1977-2010 and period of 2011-2021 over the identified sectors in Figure 3 are also tabulated in Table 1 and Table 2 respectively. It is also important to note that prior to satellite measurements starting in 1988, the measurements were done in reconnaissance missions.

Table 1. Percent Difference - 2000-2010 vs 2011-2021

Region	SW Monsoon Months		NE Monsoon Months		All-year	
	Mean	Median	Mean	Median	Mean	Median
Northern	8.86%	7.64%	0.21%	4.42%	6.00%	5.54%
Central	-7.43%	-3.06%	21.92%	20.86%	18.27%	17.82%
Southern	-9.85%	-7.84%	42.95%	32.88%	31.11%	22.10%

Table 2. Percent Difference - 1977-2010 vs 2011-2021

Region	SW Monsoon Months		NE Monsoon Months		All-year	
	Mean	Median	Mean	Median	Mean	Median
Northern	-1.58%	-2.33%	-18.95%	-20.74%	-3.66%	-3.06%
Central	-20.41%	-20.21%	-10.23%	-12.94%	-5.11%	-7.45%
Southern	-15.29%	-9.80%	-5.17%	-13.42%	-3.72%	-9.40%



3.4. Changes in the Return Period Winds

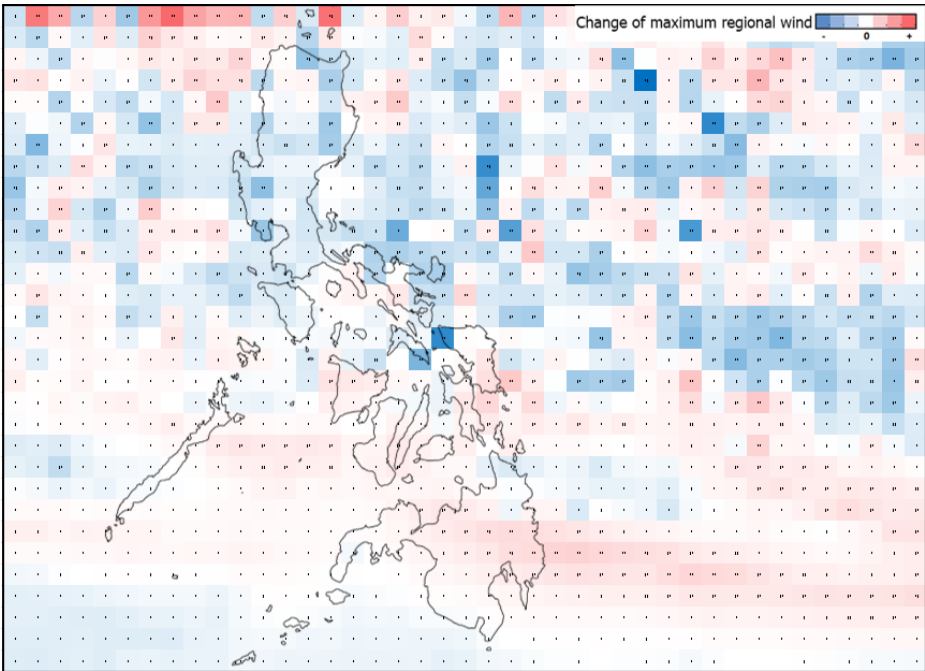


Figure 11. Change in the 100-year winds

The changes in the 100-year winds from the observation period of 1977-2010 to the observation period of 1977-2021 are also shown in Figure 11. The percent changes over the identified sectors in Figure 3, on the other hand, are tabulated in Table 3.

Table 3. Percent Change in the 100-year winds from up to 2010 to up to 2021.

Region	Change in 100-year winds	
	Mean	Median
Northern	-0.30%	-1.87%
Central	-0.62%	-0.67%
Southern	2.21%	1.94%

4. Discussion

It is important to subdivide the duration of observation into four periods: (1) the reconnaissance era by the Joint Typhoon Warning Center from 1977-1987, (2) the satellite era by the Joint Typhoon Warning Center from 1988-1999, (3) the first eleven years of Japan Meteorological Agency in the new millennium from 2000-2010, and (4) recent eleven years of the Japan Meteorological Agency from 2011-2021. The reconnaissance era is noted by the huge variations of the computed Holland-B parameters (Figure 6) showing possible uncertainties especially when relating the maximum winds to the minimum central pressure and its pressure gradient. The satellite era is noted by lesser variations in the computed Holland-B parameters as accuracy up to the regional level (free from surface friction and turbulent effects) is ensured due to the wider scope of measurement.

The Holland-B parameters, when related to the SOI, revealed that typhoons with high pressure gradients are often present during the ENSO neutral phase. El Niño allows typhoons to gather strength farther at sea but would be unable to reach the sea just east of the Philippines where intensification and rapid intensification normally occurred. La Niña on the other hand brings typhoon cyclogenesis closer to the Philippines but as a result, there will not be a longer distance to pick up strength. The neutral phase balances

the two phenomena, resulting in the typhoon having enough distance to pick up strength a little farther at sea while at the same time allowing itself for more intensification as it approaches the Philippines.

The recent eleven (11) years (2011-2021) have been noted to have stronger maximum winds compared to the eleven (11) years prior (2000-2010). Although when compared to the 34 years prior instead (1977-2010), the changes aren't that prominent especially for Northern Philippines. It is important to take note that there may be slight changes in the estimation technique within the said period, most notably with the measurements done using reconnaissance missions prior to 1988.

Evaluating the seasonal maxima shows that during the Southwest Monsoon season, there is an increase in the wind hazard in the Northern Sector of the Philippines with the exposure to the wind hazard shifting northward. During the Northeast Monsoon season, on the other hand, an increase in the wind hazard in the Southern Sector of the Philippines is observed with the exposure to the wind hazard shifting southward. Overall, the changes in the year-round maxima by comparing the maxima during the period of 2011-2021 to the maxima during the period of 2000-2010, also indicates that there is an overall increase in the wind hazard across the Philippines.

As to what to expect with the future wind hazard, the extreme values analyses determines that there will be an increase in the 100-year winds for the Southern sector of the Philippines, while the time history of the Holland-B parameters show an increasing trend since 2011, indicating that strong typhoons with higher pressure gradient and maximum sustained winds are to be expected in the future.

5. Conclusions

There has been an overall increase of typhoon strength over the years. Climate change results in typhoons having more violent winds with steeper pressure gradients near the center especially during the ENSO neutral phase. The wind hazard has also shifted spatially with the Southern sectors of the Philippines or the Southern Philippines in general being more susceptible to typhoons in recent years. The Southern Philippines experiences an increase (decrease) of wind hazard during the Northeast (Southwest) Monsoon season. The Northern Philippines experiences an increase (decrease) of wind hazard during the Southwest (Northeast) Monsoon season. The overall increase in both the historical maximum and the return period wind should prompt an update to the wind design to meet the demand of these noted increases in order to ensure that the updated building design will achieve sustainability.

Supplementary Materials: The following supporting information can be downloaded at: www.mdpi.com/xxx/s1, Figure S1: Maximum Regional Cyclonic Winds – Southwest Monsoon Season (2000-2010); Figure S2: Maximum Regional Cyclonic Winds – Southwest Monsoon Season (2011-2021); Figure S3: Maximum Regional Cyclonic Winds – Southwest Monsoon Season (1977-2010); Figure S4: Maximum Regional Cyclonic Winds – Southwest Monsoon Season (1977-1987); Figure S5: Maximum Regional Cyclonic Winds – Southwest Monsoon Season (1988-2010); Figure S6: Maximum Regional Cyclonic Winds – Northeast Monsoon Season (2000-2010); Figure S7: Maximum Regional Cyclonic Winds – Northeast Monsoon Season (2011-2021); Figure S8: Maximum Regional Cyclonic Winds – Northeast Monsoon Season (1977-2010); Figure S9: Maximum Regional Cyclonic Winds – Northeast Monsoon Season (1977-1987); Figure S10: Maximum Regional Cyclonic Winds – Northeast Monsoon Season (1988-2010); Figure S11: Maximum Regional Cyclonic Winds – Year-round (2000-2010); Figure S12: Maximum Regional Cyclonic Winds – Year-round (2011-2021); Figure S13: Maximum Regional Cyclonic Winds – Year-round (1977-2010); Figure S14: Maximum Regional Cyclonic Winds – Year-round (1977-1987); Figure S15: Maximum Regional Cyclonic Winds – Year-round (1988-2010); Figure S16: 100-year winds (1977-2010); Figure S17: 100-year winds (1977-2021);

Author Contributions: Conceptualization, J.C.A.; methodology, J.C.A.; software, J.C.A.; analysis, J.C.A.; investigation, J.C.A.; data curation, J.C.A.; writing—original draft preparation, J.C.A.; writing—review and editing, J.C.A.; visualization, J.C.A..The author read and agreed to the published version of the manuscript

Data Availability Statement: The detailed wind information data from Japan Meteorological Agency can be obtained through <http://agora.ex.nii.ac.jp/digital-typhoon/>

Acknowledgments: To my future wife, Kimberly Buenaobra for her constant support. To my friends Timothy James Cipriano and Kevin Cordoviz who made the appraisal to this research. To the Structural Engineering Group faculty, for the support and encouragement.

Institutional Review Board Statement: Not applicable

Informed Consent Statement: Not applicable

Conflicts of Interest: The author declares no conflict of interest.

References

1. Cinco, T.; de Guzman, R.; Ortiz, A.; Delfino, R.; Lasco, R.; Hilario, F.; Juanillo, E.; Barba, R.; Ares, E. Observed trends and impacts of tropical cyclones in the Philippines. *International Journal of Climatology* 2016, 36, 4638–4650.
2. Bueza, M. Storm signal no. 4 in PH history <https://www.rappler.com/newsbreak/iq/43058-storm-signal-number-ph-history/#:~:text=To%20classify%20more%20powerful%20storms,4>.
3. Storm Signal No. 5 officially added by PAGASA <https://www.cnnphilippines.com/news/2015/05/21/PAGASA-adds-Signal-No-5.html>.
4. Philippine Atmospheric, Geophysical, and Astronomical Services Administration *DOST-PAGASA MODIFIES TROPICAL CYCLONE WIND SIGNAL (TCWS) SYSTEM*; 2022.
5. Kyoto Protocol to the United Nations Framework Convention on Climate Change, Dec. 10, 1997 37 I.L.M. 22 (1998); 2303 U.N.T.S. 148; U.N. Doc FCCC/CP/1997/7/Add.1
6. Paris Agreement to the United Nations Framework Convention on Climate Change, Dec. 12, 2015, T.I.A.S. No. 16-1104
7. Griggs, D.; Noguer, M. Climate change 2001: The scientific basis. Contribution of Working Group I to the Third Assessment Report of the Intergovernmental Panel on Climate Change. *Weather* 2002, 57, 267–269.
8. Giorgi, F.; Hewitson, B.; Christensen, J.; Hulme, M.; and 5 others. Regional climate change information — evaluation and projections. In: Houghton JT, Ding Y, Griggs DJ, Noguer M, van der Linden PJ, Xiaosu D (eds) Climate change 2001 – the scientific basis. Cambridge University Press, Cambridge and New York, 2001. p.583–638
9. Walsh, K. Tropical cyclones and climate change: unresolved issues. *Climate Research* 2004, 27, 77–83.
10. Katzfey, J. Tropical Cyclones and Climate Change Predictions In *Asia Pacific Conference of Wind Engineering*; 2017.
11. Black, R.; Hallett, J. Observations of the Distribution of Ice in Hurricanes. *Journal of the Atmospheric Sciences* 1986, 43, 802–822.
12. Cha, E.; Knutson, T.; Lee, T.; Ying, M.; Nakaegawa, T. Third assessment on impacts of climate change on tropical cyclones in the Typhoon Committee Region – Part II: Future projections. *Tropical Cyclone Research and Review* 2020, 9, 75–86.
13. Walsh, K.; Camargo, S.; Knutson, T.; Kossin, J.; Lee, T.; Murakami, H.; Patricola, C. Tropical cyclones and climate change. *Tropical Cyclone Research and Review* 2019, 8, 240–250.
14. Tierra, M.; Bagtasas, G. Identifying the rapid intensification of tropical cyclones using the Himawari-8 satellite and their impacts in the Philippines. *International Journal of Climatology* 2022.
15. Basconcillo, J.; Moon, I. Recent increase in the occurrences of Christmas typhoons in the Western North Pacific. *Scientific Reports* 2021, 11.
16. Cordoviz, K.C. Influence of the West Pacific Subtropical High on Landfalling Winter Tropical Cyclones in the Philippines. Master's Thesis, University of the Philippines, Quezon City, 17 May 2022.
17. Racoma, B.; Klingaman, N.; Holloway, C.; Schiemann, R.; Bagtasas, G. Tropical cyclone characteristics associated with extreme precipitation in the northern Philippines. *International Journal of Climatology* 2021, 42, 3290–3307.
18. Zhou, T.; Yu, R.; Zhang, J.; Drange, H.; Cassou, C.; Deser, C.; Hodson, D.; Sanchez-Gomez, E.; Li, J.; Keenlyside, N.; Xin, X.; Okumura, Y. Why the Western Pacific Subtropical High Has Extended Westward since the Late 1970s. *Journal of Climate* 2009, 22, 2199–2215.
19. Wang, B.; Xiang, B.; Lee, J. Subtropical High predictability establishes a promising way for monsoon and tropical storm predictions. *Proceedings of the National Academy of Sciences* 2013, 110, 2718–2722.
20. Agar, J.; Acosta, T.; Hernandez, J. Regional Cyclonic Wind Field Modeling in the Philippines. In *17th Engineering Research and Development for Technology Conference*; 2021.
21. Schloemer, R.. Synthesis of Hurricane Winds over Lake Okeechobee. In *Analysis and Synthesis of Hurricane Wind Patterns Over Lake Okeechobee, Florida*, Hydrometeorological Report No. 31.; U.S. Department of Commerce Weather Bureau: Washington D.C., USA, 1954; pp. 154–196.
22. Holland, G.; Belanger, J.; Fritz, A. A Revised Model for Radial Profiles of Hurricane Winds. *Monthly Weather Review* 2010, 138, 4393–4401.

-
23. Holland, G. An Analytic Model of the Wind and Pressure Profiles in Hurricanes. *Monthly Weather Review* 1980, *108*, 1212-1218.
 24. World Meteorological Organization. The Beaufort Scale of Wind Force : (Technical and Operational Aspects). Commission for Maritime Meteorology. Geneva : WMO, 1970.
 25. Harper, B.; Kepert, J., and Ginger, J. Guidelines for converting between various wind averaging periods in tropical cyclone conditions. *World Meteorological Organization* 2010.
 26. Gumbel, E.J. Statistical theory of extreme values and some practical applications. *Applied Math Series* 1954, 33.
 27. Holmes, J.. *Wind Loadings on Structures*, 1st ed.; Taylor and Francis Group: United Kingdom, 2001; pp. 31.
 28. Southern Oscillation Index (SOI) and Equatorial SOI http://iridl.ldeo.columbia.edu/maproom/ENSO/Time_Series/Equatorial_SOI.html.
 29. Southern Oscillation Index | El Niño/Southern Oscillation (ENSO). <https://www.ncei.noaa.gov/access/monitoring/enso/soi>